Available online at www.sciencedirect.com
SCIENCE DIRECT®
Cement & Concrete Composites 27 (2005) 583–592
Cement & Concrete Composites
www.elsevier.com/locate/cemconcomp

Microstructure and mechanical properties of waste fibre–cement composites

H. Savastano Jr. [a,*], P.G. Warden [b], R.S.P. Coutts [c]

[a] University of São Paulo, P.O. Box 23, 13635-900 Pirassununga, SP, Brazil
[b] CSIRO, Forestry and Forest Products, Private Bag 10, Clayton South, Vic. 3169, Australia
[c] Assedo Pty. Ltd., 75 Sandringham Rd, Vic. 3191, Australia

Abstract

This paper examines the microstructure of composite materials containing fibrous wastes (as reinforcement in granulated blast furnace slag or ordinary Portland cement matrices). Both secondary and back-scattered electron imaging and energy dispersive X-ray spectroscopy were used for compositional analysis. Evaluation of both fractured and cut surfaces provided the morphological and bonding information that was related to mechanical performance obtained from flexural tests. Sisal and *Eucalyptus grandis* pulps showed satisfactory bonding to the cement matrix, with fibre pullout predominating as indicated by high values of energy absorption. In contrast banana pulp reinforced composites exhibited fibre fracture as the main failure mechanism. In all analysed composites, partial fibre debonding and matrix micro-cracking were dominant at the interfaces. However, there was no evidence of a porous transition zone or massive concentration of calcium hydroxide at the interface.

Keywords: Microscopy; Waste materials; Sisal fibre; Banana fibre; *Eucalyptus grandis* fibre; *Pinus radiata* fibre; Fibre–cements

1. Introduction

The use of waste fibres as reinforcement in cement composites has enormous potential in the field of recycled materials for civil construction. The optimised recycled composites present an acceptable behaviour in comparison with fibre cement produced with virgin wood cellulose fibres [1]. The availability of non-commercial fibrous wastes also supports their potential utilization throughout sustainable methods of production of building components [2]. Granulated blast furnace slag (BFS) proved to be an adequate binder for vegetable fibre reinforcement in low cost housing [3]. The lower alkalinity of BFS compared to that of commercial ordinary Portland cement (OPC) can be advantageous, with respect to the long-term durability of natural fibre–reinforced cement products. The slurry vacuum de-watering process of fabrication, followed by pressing and air-curing, provides composites with outstanding mechanical and physical performance, when compared with conventional dough mixing methods [4]. The microscopic material response for different processing types can be evaluated by comparing results presented in the literature [5–7]. The vacuum de-watering/press consolidation method was associated with a cellulose fibre–cement transition zone with reduced incidence of high porosity and portlandite macro-crystals. The water/binder ratio, porosity of composite, fibre morphology and matrix compaction were shown to play key roles in the resultant fibre–matrix interfacial bond in cellulose fibre–cement based materials [7].

The objective of the present study was to examine the microstructure of waste fibre–cement composites bonded with BFS and OPC matrices. Fracture surfaces indicated whether fibre fracture or fibre pullout occurred

* Corresponding author. Fax: +55 1935 6541 14.
E-mail address: holmersj@usp.br (H. Savastano Jr.).

0958-9465/$ - see front matter © 2004 Elsevier Ltd. All rights reserved.
doi:10.1016/j.cemconcomp.2004.09.009

during bending to failure. Cut and polished surfaces were also prepared to view the transition zone. Compositional analyses were performed in the fibre–matrix interfacial areas.

2. Experimental

2.1. Materials

Two different types of binder were tested for cement paste matrix production:

- Alkaline granulated iron blast-furnace slag (BFS) (glass content = 99.5% in mass, 500 m^2/kg Blaine fineness), activated by gypsum and lime. Table 1 shows the chemical composition of the BFS used in this work, which was the same material studied by Oliveira et al. [8].
- Commercial ordinary Portland cement—Adelaide Brighton brand type GP (Australian Standard AS 3972 1991)—assumed to contain less than 5% of mineral additions.

The following waste fibrous materials originated from Brazil: sisal (*Agave sisalana*) field by-product, banana (*Musa cavendishii*) pseudo-stem strand fibre and *Eucalyptus grandis* waste pulp from both kraft cooking and bleaching mill stages. Banana and sisal raw materials were kraft cooked following previous studies by Zhu et al. [9] and Coutts and Warden [10]. *Eucalyptus grandis* pulp was used in the as received condition, i.e. after fibre dispersion by hot water disintegration.

Chopped strand fibres of commercial sisal and also *Pinus radiata* beaten kraft lap pulp were used as controls and provided links with earlier studies carried out both in Brazil [11] and in Australia [4]. The main physical properties of the fibres were determined and are reported in Table 2. Although possessing similar aspect ratios, the cellulose pulps presented micro-fibres in comparison with the chopped strands of commercial sisal. *Eucalyptus grandis* presented an average length considerably shorter than the other kraft pulps, this being characteristic of hardwood and waste fibres. The cement composites reinforced with pulped fibres were prepared using a slurry (between 20% and 30% of solids by mass) vacuum de-watering process, pressed at 3.2 MPa for 5 min, and cured in saturated air for 7 days. They were then maintained in an environment of 23 ± 2 °C and 50 ± 5% relative humidity until tested under the same conditions at 28 days of age. Further information related to the analysed composites is presented in Table 3. This includes physical and mechanical properties after curing for 28 days. The methodology used for composite preparation, conditioning and mechanical testing is the same as that detailed in an analogous study conducted by Eusebio et al. [12]. In the case of strand sisal reinforced composites, instead of slurring, the formulation was mixed for 5 min in a heavy-duty dough mixer using a 0.40 water–cement ratio, the remaining steps being kept constant. For all formulations, the fibre content was restricted to 4% by mass of binder (approximately 5% of composite volume) to assist microscopy observations. The excessive incidence of filaments could increase difficulties in coating the specimens, achieving acceptable depth of field and eliminating charges from the electron beam in the scanning electron microscopy.

Table 1
Chemical composition of granulated blast furnace slag (% by mass)

Loss on ignition	1.67	Na_2O	0.16
SiO_2	33.78	K_2O	0.32
Al_2O_3	13.11	S^{2-}	1.14
Fe_2O_3	0.51	Free CaO	0.1
CaO	42.47	Insoluble residue	0.53
MgO	7.46	CO_2	1.18
SO_3	0.15		

Table 2
Pulp and fibre properties

Fibre	Pulp and refining processes	Length (mm)[a]	Width (μm)[b]	Aspect ratio
Pinus radiata	Beaten kraft	1.71	32.4	53
Commercial sisal	Unpulped slivers	12	135	89
By-product sisal	Kraft	1.66	13.5	123
Banana	Kraft	1.95	15.3	127
Eucalyptus grandis waste	Kraft	0.66	10.9	61

[a] Kajjani FS-200 automated optical analyser.
[b] Average of 20 determinations by SEM.

2.2. Microscopy

Specimens were analysed at different ages using a Philips XL30 field emission gun (FEG) scanning electron microscope (SEM). A secondary electron (SE) detector, operated at 5.0 kV accelerating voltage, was chosen for the analysis of the fractured surfaces of flexural test specimens (loading rate of 0.5 mm/min, sample thickness ~6 mm and span 100 mm). For obtaining improved views of the fibres, some images were taken after tilting the samples 75° in relation to the horizontal plane. These procedures were in accordance with Coutts and Kightly [13].

The back-scattered electron (BSE) detector at 15.0 kV was applied for viewing cut and polished surfaces. As reported elsewhere [14,15], a BSE image permits easy identification of composite phases by way of atomic number contrast. The BSE imaging was used to study the fibre–matrix transition zone.

Energy dispersive X-ray spectroscopy (EDS) analyses were also conducted. These were performed on the same

Table 3
Composites description and properties

Fibre		Binder composition	Mechanical properties (28 days)[a]		Physical properties (28 days)[a,b]		
Type	Content (% of binder mass)		Flexural strength (MPa)	Toughness (kJ/m^2)	Water absorption (% by mass)	Density (g/cm^3)	Permeable voids (% by volume)
Pinus radiata beaten kraft	4	100% OPC	19.20 ± 1.90	0.64 ± 0.09	18.5 ± 0.5	1.69 ± 0.02	31.1 ± 0.5
Commercial sisal slivers	4	100% OPC	14.40 ± 1.00	0.58 ± 0.17	14.9 ± 0.7	1.86 ± 0.04	27.8 ± 0.8
By-product sisal kraft	4	100% OPC	16.50 ± 0.60	0.39 ± 0.06	17.9 ± 0.3	1.70 ± 0.01	30.5 ± 0.5
	4	92% BFS, 6% gypsum, 2% lime	13.10 ± 0.40	0.53 ± 0.12	26.6 ± 0.5	1.50 ± 0.01	39.7 ± 0.6
Banana kraft	4	100% OPC	15.50 ± 1.30	0.21 ± 0.03	16.5 ± 0.2	1.71 ± 0.02	28.2 ± 0.3
Eucalyptus grandis waste kraft	4	100% OPC	15.50 ± 0.80	0.29 ± 0.04	16.8 ± 0.8	1.78 ± 0.03	29.8 ± 0.8
	4	88%BFS, 10% gypsum, 2% lime	14.30 ± 0.89	0.25 ± 0.02	23.9 ± 1.2	1.58 ± 0.04	37.7 ± 0.9

[a] Average ± single standard deviation.
[b] ASTM C948-81.

flat surface specimens in an effort to obtain semi-quantitative compositional information. For the applied accelerated voltage (15.0 kV) and material densities between 1.5 and 2.0 g/cm^3, each spot analysis can be interpreted as an average composition in a bulb region with a diameter less than 4 μm.

The preparation of specimens for BSE and EDS began with vacuum (~60 kPa gauge) impregnation using epoxy (Araldite "M" and hardener "HY 956" in 100:20 mass proportion) diluted in ethanol (20% of total resin mass). The initial cure was conducted at room temperature, after which the specimens were placed in a 40 °C oven until complete polymerisation had occurred. Surface lapping was carried out with silicon carbide abrasive paper (sizes 37 μm, 25 μm and 13 μm in this sequence for 5 min each). Polishing operations used in turn 6 μm, 1 μm and 0.1 μm diamond polishing compound (20 min each size). Every lapping and polishing step intercalated with acetone ultrasonic bath for cleaning and finally specimens were vacuum carbon coated before microscopy sessions. The presented preparation was based on the recommendations of Kjellsen et al. [16]. It should be noted that composite microstructures were examined at ages greater than 28 days and some changes from those existing at the time of physical and mechanical testing would be expected to have occurred.

3. Results and discussion

3.1. Polished surface observations

Sisal slivers in OPC can be easily identified in BSE images (Fig. 1) as dark grey phases, differing from hydration products (medium grey area) and from denser un-hydrated cement grains (light grey). Loss of bonding was prominent, as the slivers shrunk strongly upon drying. Matrix cracking also occurred close to the fibres, as a result of internal tensile stresses generated by volume changes in the fibres.

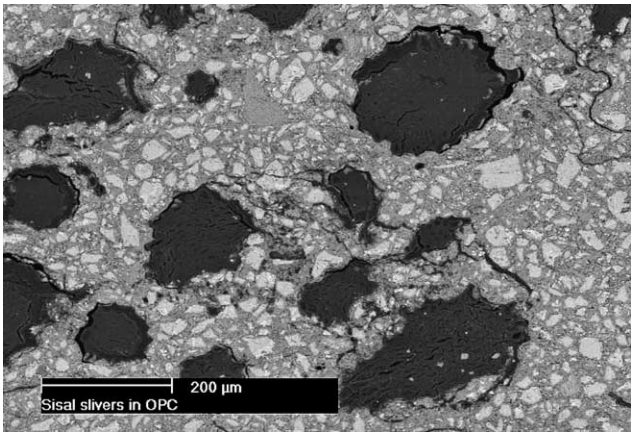

Fig. 1. BSE image of 149 days old 4% sisal slivers in OPC.

The considerable capacity of water absorption (~100% by mass) of slivers increases the water/cement ratio of the cement paste in the vicinity of the fibre. As a consequence, the differential drying shrinkage of OPC matrix can also generate cracks close to the fibre–cement interface.

However, no porous transition zone could be clearly defined in Fig. 1, contrary to the report by Savastano Jr. and Agopyan [5] of a sisal sliver–cement transition zone that was about 200 μm thick at 180 days. The major explanation for such a different behaviour in the present

study could be the use of vacuum de-watering and high pressure applied to the composite straight after moulding. As proposed by Coutts [7] the specified procedures increase the composite compaction and reduce the water–cement ratio. Besides compressible and permeable vegetable fibres are likely to absorb excess water when the pressure is released.

The ribbon shape of *Pinus radiata* beaten fibres can be attested to in Fig. 2. Partial debonding and cracks occurred, and no fibre mineralisation was indicated by EDS analysis of lumen area (spot 1 of Fig. 2 related to Fig. 3 compositional spectrum) at 251 days. Spot 2 of Fig. 2 identified a high incidence of calcium hydroxide close to the fibre surface (see EDS spectrum in Fig. 4). Although the formation of free lime is associated with the hydration of OPC [17], this massive concentration of portlandite was not common in other EDS observations. Therefore, it was not considered as a preferential deposition of this hydration product in the fibre surface.

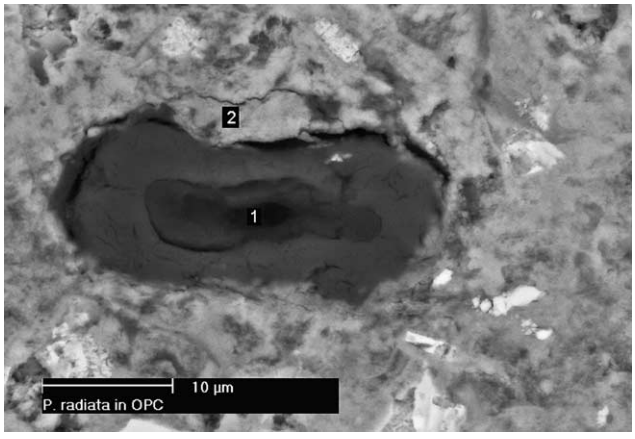

Fig. 2. BSE image of 251 days old cross-sectioned *Pinus radiata* in OPC. Spot 1 lumen; spot 2: hydration products at fibre surface.

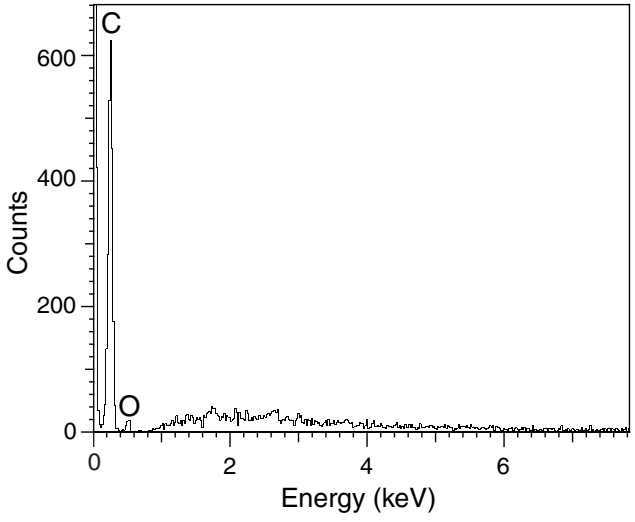

Fig. 3. EDS spectrum of *Pinus radiata* internal lumen (spot 1 in Fig. 2).

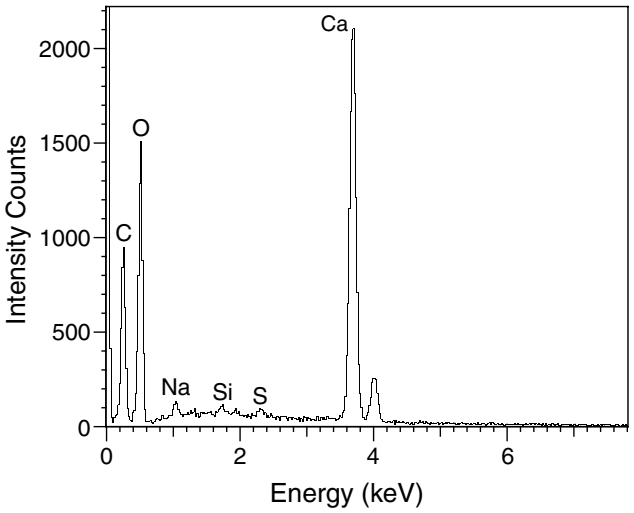

Fig. 4. EDS spectrum of *Pinus radiata*–OPC interfacial region rich in calcium hydroxide (spot 2 in Fig. 2).

Kraft pulped sisal by-product presented good contact area in the OPC matrix performing total fibre perimeter about 10 times larger (mathematical assumption upon the average fibre diameter) than the corresponding slivers. This comparison was taken from Figs. 1 and 5a, keeping in mind that the fibres represented approximately 20% of observed surface in both figures (as determined by an image analyser).

Higher magnifications of sisal kraft in OPC and BFS are depicted in Figs. 5(b) and 6, respectively. The circle like cross-section of individual filaments and/or the open internal lumen are characteristics of unbeaten kraft pulps. Fibres like those are known to be less conformable and have inferior packing ability when used in the Hatschek production process [1,4].

Further observation of Figs. 5(b) and 6 revealed dense fibre–cement interfacial areas and partial fibre debonding similar to Fig. 1 (sisal slivers in OPC), although, with a 20 times scale difference. No calcium hydroxide rich transition zones were identified by spot analyses close to the fibres ('X' marks in Figs. 5(b) and 6). The EDS analyses following in Figs. 7 and 8 detected chemical elements normally present in cement hydration products with calcium–silica count ratios between 1.3 and 2.0.

In contrast to the OPC composite (Fig. 5(b)), BFS un-hydrated grains presented sharp edges and reduced surface attack, as indicators of low chemical reaction. Future studies should consider more effective chemical–thermal catalyses for the improvement of BFS mechanical performance.

Longitudinal views of banana fibre in OPC (Fig. 9) and *Eucalyptus grandis* in BFS (Fig. 10) show the main characteristics of the transition zones in the composites:

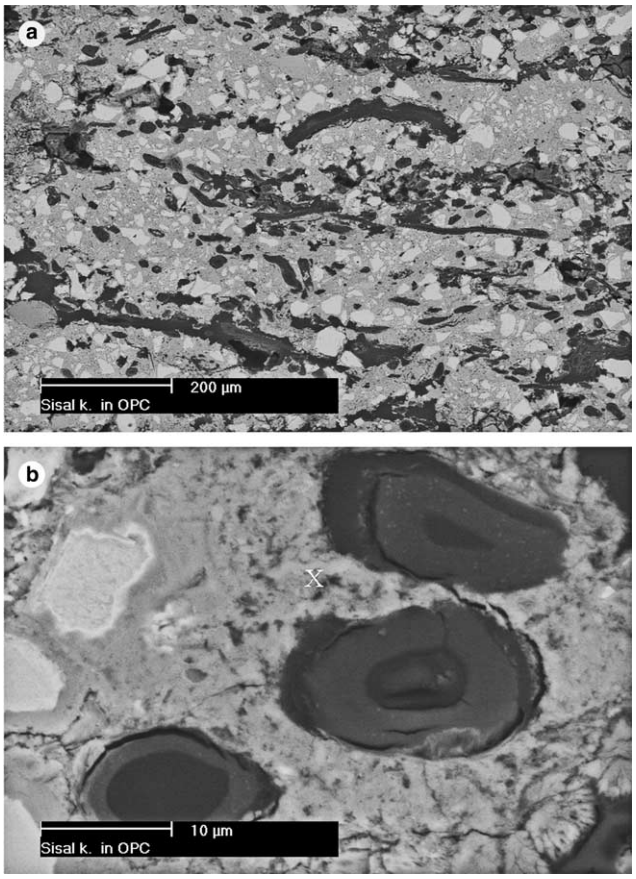

Fig. 5. BSE image of 237 days old 4% sisal kraft in OPC. (a) General view. (b) Detail of cross-sectioned sisal filaments. 'X' mark refer to EDS analysis at Fig. 7.

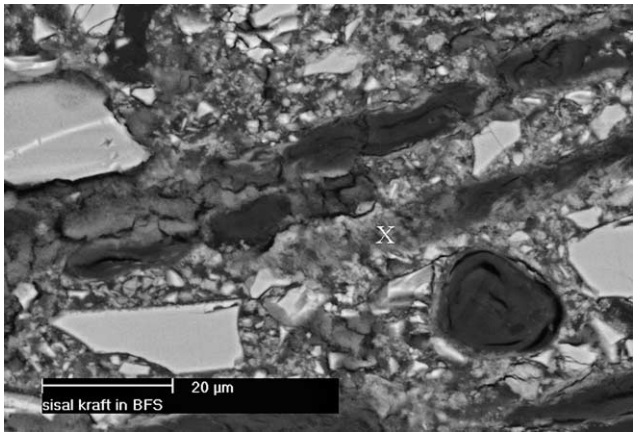

Fig. 6. BSE image of 236 days old sisal kraft in BFS. 'X' mark refer to EDS analysis at Fig. 8.

partial bonding and matrix micro-cracking, but no localised high porosity at the ages that were studied.

Fig. 11 depicts an EDS analysis connected to area '1' in Fig. 9, which was an un-hydrated cement grain rich in di-calcium silicate (Ca/Si = 1.7). Fig. 12 is associated with spot '2' of the same BSE image, close to the fibre

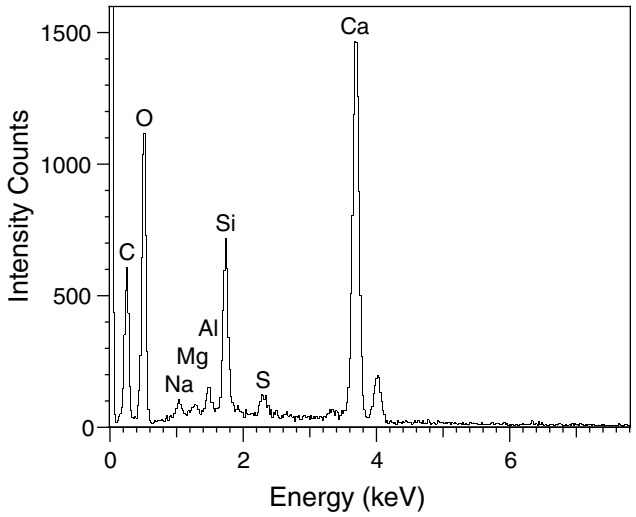

Fig. 7. EDS spectrum of sisal kraft in OPC close to fibres with evidence of ettringite and tobermorite related phases ('X' spot in Fig. 5(b)).

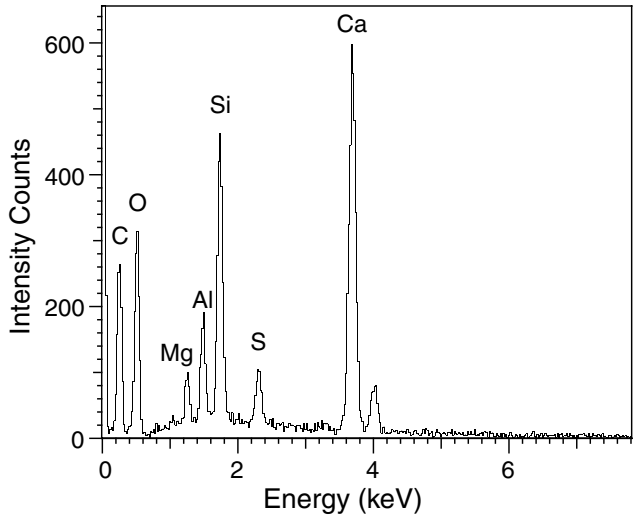

Fig. 8. EDS spectrum of hydration products in sisal kraft-BFS composite ('X' spot in Fig. 6).

surface. In this case, the presence of hydration products (Al–S related and Ca/Si ~3.0) agreed with general EDS determinations (e.g. Figs. 7 and 8). There was no evidence of massive free lime close to the fibres.

Fig. 13 shows *Eucalyptus grandis* in OPC at identical magnification to those of Figs. 1 and 5(a). Again, it shows the advantage of pulped fibres in generating a high contact area with the matrix. *Eucalyptus grandis* waste fibres are more homogeneously distributed than the sisal by-product kraft.

As a general observation BFS based composites performed similarly to OPC ones when reinforced with cellulose fibres in view of the bonding characteristics in the interfacial areas and correspondent EDS results. The reduction of capillary permeability can be a future

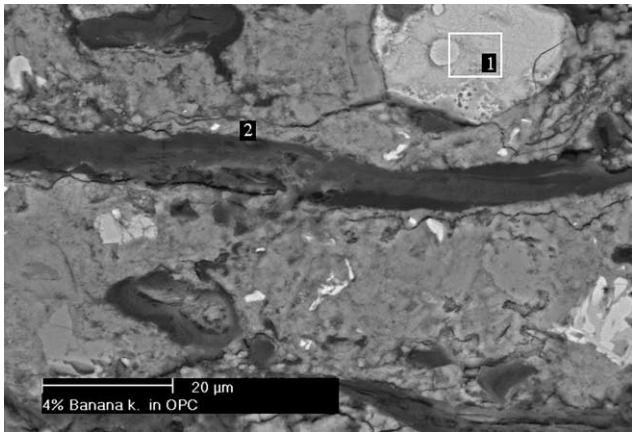

Fig. 9. BSE image of 151 days old banana fibre longitudinal section in OPC. Area 1: un-hydrated cement grain; spot 2: hydration products at fibre surface.

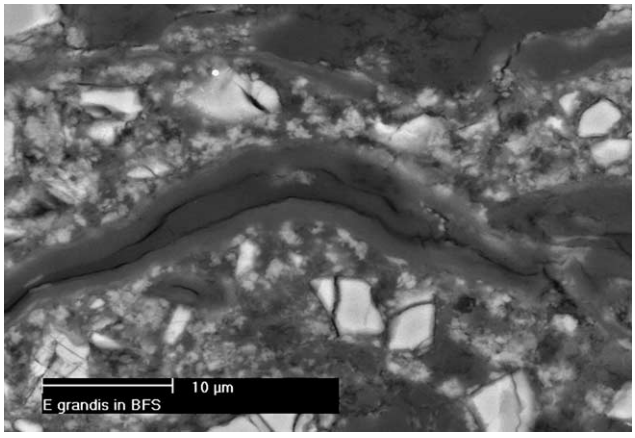

Fig. 10. BSE image of 83 days old *Eucalyptus grandis* longitudinal section in BFS.

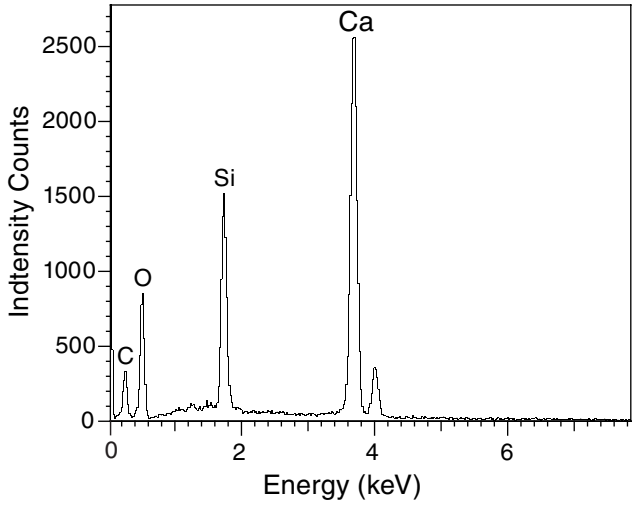

Fig. 11. EDS spectrum of un-hydrated cement grain related to area 1 in Fig. 9.

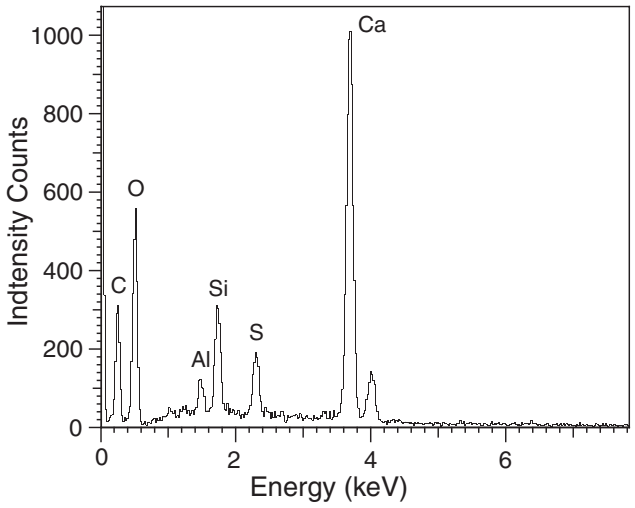

Fig. 12. EDS spectrum of hydrated OPC close to banana fibre surface (spot 2 in Fig. 9).

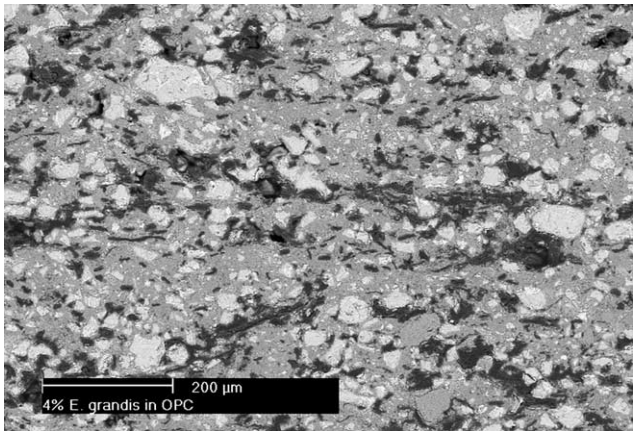

Fig. 13. BSE image of 171 days old 4% *Eucalyptus grandis*–OPC composites.

valuable step in the improvement of mechanical performance of BSF based composites. The improved packing of the matrix combined with the more effective activation of BFS could be a reasonable action to obtain composites with higher densities.

3.2. Fracture surface observations

The *Pinus radiata* beaten kraft in OPC matrix achieved the best results of flexural strength and toughness compared with other 4% fibre content composites (Table 3) in this study. As showed in Fig. 14, the fibres presented lateral shrinkage as characteristic of dried lap pulps [18]; also flat shape and low aspect ratio (=53 and significantly below the 80–100 range reported by Coutts [4]) should be associated to fibre damage as consequence of previous refinement. In accordance with description by Coutts and Kightly [13] for similar composites, frac-

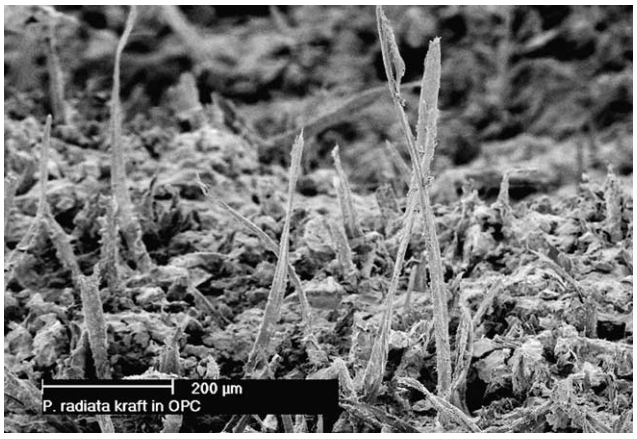

Fig. 14. SE image (75° tilt, gold coat) of 240 days old 4% *Pinus radiata* beaten kraft in OPC.

ture and fibre pullout co-exist providing a desirable fibre–matrix bond level leading to both good flexural strength and toughness. This ideal behaviour is likely to happen for fibres close to the critical length, which depends on fibre and matrix characteristics. Twisting as indicative of fibre internal collapse, incrustation of matrix at fibres surface and fractured ends of pulled out filaments were all indications of both phases working together to provide effective fibre reinforcement.

Fig. 15 depicts sisal slivers in OPC and it is possible to observe individual fibres in bundles with low specific contact area inside the matrix. The fibre aspect ratio is 89 (see Table 2). This limited length of anchorage helps to explain fibre pullout predominance and toughness values of the same magnitude of the composites reinforced with pulped fibres. On the other hand one should be aware of the slivers high stiffness, resulting in difficult dispersion within the matrix. It was found that 4% content of strands in OPC was the highest amount that could be introduced during the dough mixing, whereas, pulped fibres are usually able to be introduced up to 14% content, depending on the fibre length, with significant improvement in mechanical properties. As an example, Coutts and Warden [10] reported flexural strength up to 18 MPa and toughness of 2.5 kJ/m^2 for air-cured cement mortars containing 8% by mass of kraft sisal fibre produced in similar way to the present study. Ageing is also an important approach, since individual filaments are linked to each other by lignin that could be easily decomposed in alkali media. It means considerable loss of mechanical properties should be expected during the lifetime of vegetable sliver-reinforced OPC based material [19].

Kraft pulped sisal by-product fibres as reinforcement of OPC and BFS composites are depicted in Figs. 16 and 17, respectively. In both cases, the smooth surface of unbeaten long fibres provided predominantly fibre pullout. However, some fracture ended filaments indicated the good interaction between the two phases of the composites. For the BFS composite (Fig. 17), the fibre surfaces have considerable matrix material attached to them.

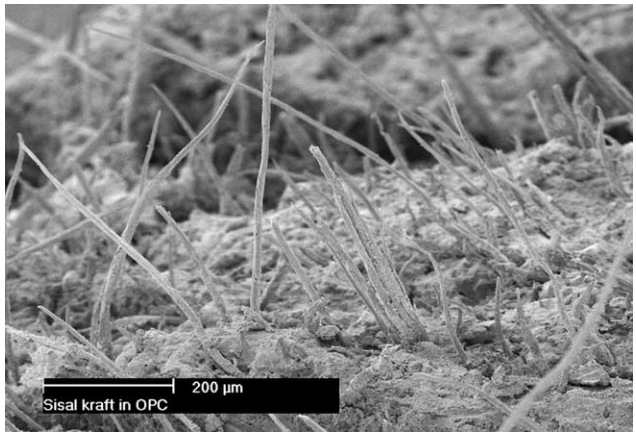

Fig. 16. SE image (75° tilt, gold coat) of 226 days old 4% sisal kraft in OPC.

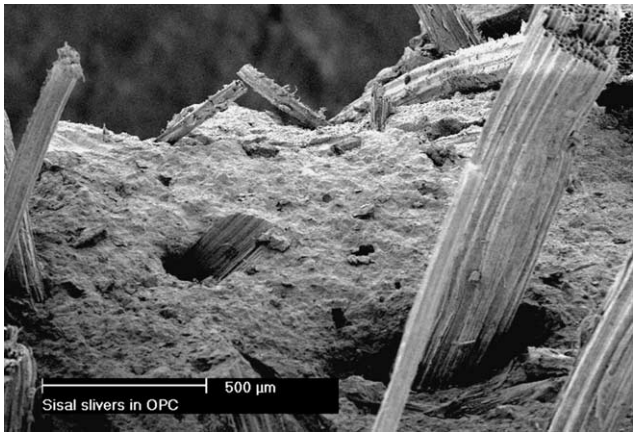

Fig. 15. SE image (75° tilt, gold coat) of 138 days old 4% sisal slivers in OPC.

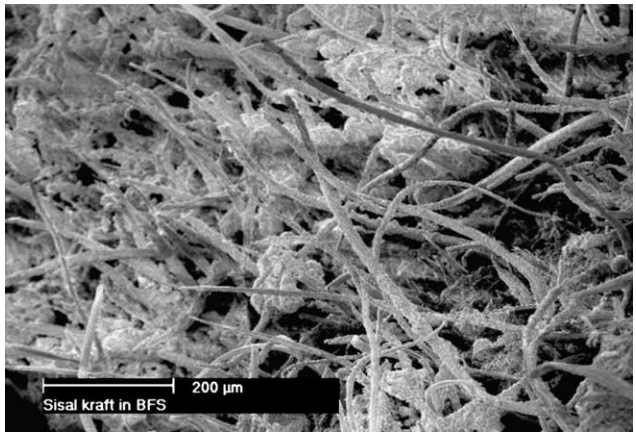

Fig. 17. SE image (75° tilt, gold coat) of 225 days old 4% sisal kraft in BFS.

This can be explained by better bonding or weaker matrix material (when compared to OPC). These characteristics were able to provide sisal BFS composites with higher energy absorption during cracking. They resulted in toughness values that were 35% higher than those of sisal in OPC.

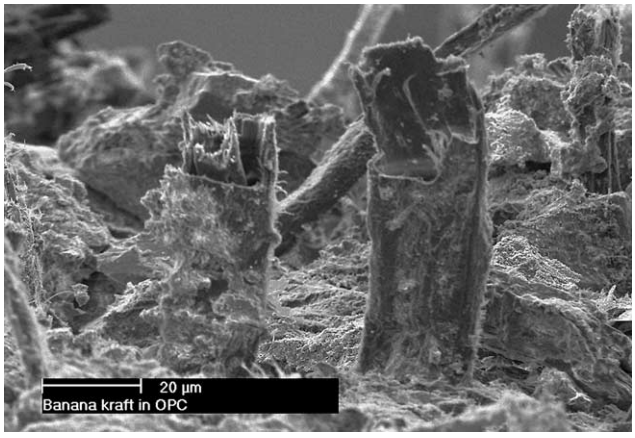

Fig. 18. SE image (75° tilt, carbon coat) of 140 days old 4% banana kraft in OPC.

The fracture surface of banana fibre reinforced OPC is depicted in Fig. 18 displaying numerous broken filaments. These long and supposedly strong fibres (tensile strength ~800 MPa, comparable to *Pinus radiata* as reported by Coutts [20]), would be expected to show considerable fibre pullout. Hence, fibre damage may have occurred during pulping or composite preparation. Consequently the composite absorbed low energy in the post-cracking stage. This was in despite of the flexural strength, which was close to that of the sisal composite. The above behaviour could be expected for air-cured aged composites [6]. However, the internal lumen of filaments appeared free from the deposition of hydration products (or fibre petrifaction).

Eucalyptus grandis waste pulp reinforced OPC (Fig. 19(a)) or BFS (Fig. 20(a)) showed higher incidence of pullout than fibre fracture, as expected for short hardwood fibres (~0.66 mm length average). On the other hand, the particular fibre in Fig. 19(b) shows matrix incrustation that suddenly changed in clean surface, which suggests removal of the outer layer of the fibre due to good adhesion between phases. In the case of BFS matrix, the fibre and cement incrustation indicate

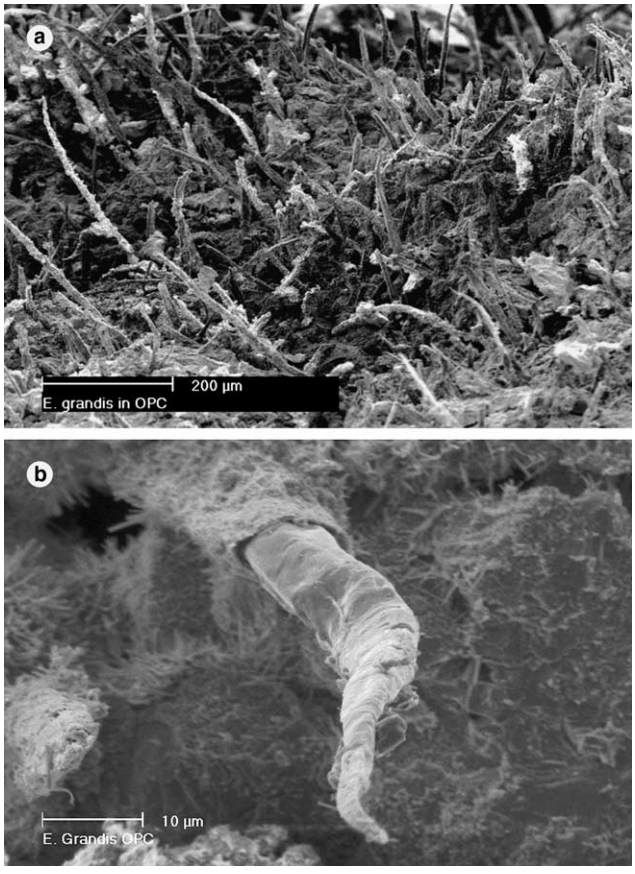

Fig. 19. SE image (carbon coat) of approximately 160 days old 4% *Eucalyptus grandis* in OPC. (a) General view (75° tilt). (b) Detail of an individual fibre (no tilt).

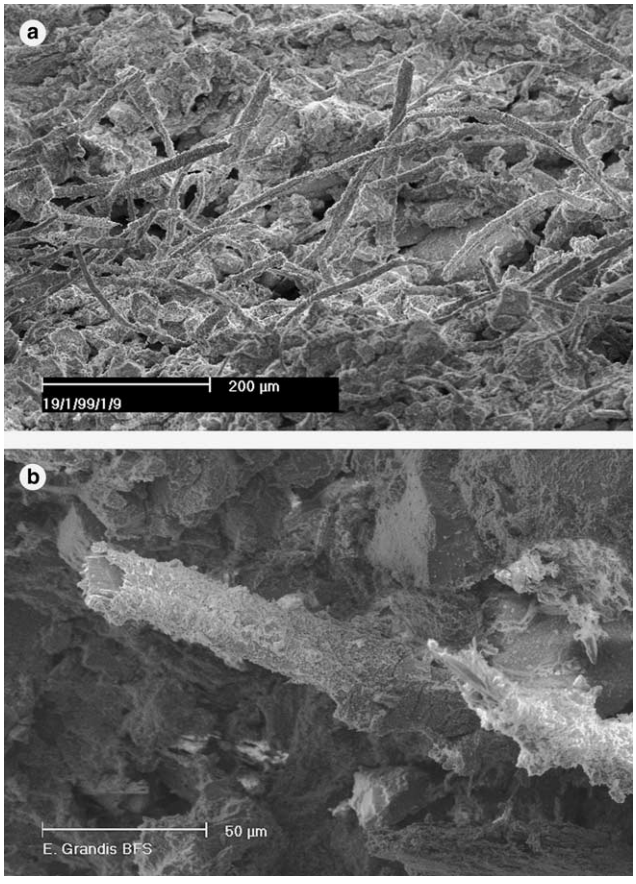

Fig. 20. SE image (no tilt) of approximately 60 days old 4% *Eucalyptus grandis* in BFS. (a) General view (no coat). (b) Detail of pulled-out fibre (carbon coat).

that the matrix may be weaker than OPC (see Fig. 20(b)). The *Eucalyptus grandis* based composites possessed better mechanical performance than those reinforced with the longer banana filaments, for fibre levels over 4% as reported elsewhere [21].

4. Conclusions

Sisal and *Eucalyptus grandis* pulped waste fibres presented satisfactory bonding either in OPC or BFS matrices. From the interpretation of SE images, pulled out fibres showing fractured extremities, outer layer removal and also matrix incrustations, all of them should be considered as indicators of tough composites.

The interfacial bonding of beaten *Pinus radiata* in OPC appeared to work near the fibre critical length providing the best mechanical performance under flexural tests amongst the studied materials.

Comparison between pulped sisal fibres and sisal slivers emphasised the advantage of individual filaments for reinforced cement pastes. Elevated stiffness, considerable volume change in wet medium and low specific contact area with matrix are limiting factors for the optimum use of slivers as cement reinforcement. Also bundles of fibres that are lignin-rich can decompose inside highly alkaline matrices.

In the case of banana kraft pulp in OPC, high aspect ratio provided greater fibre–matrix bonding with increased fibre fracture and reduced fibre pullout and hence lower toughness.

BFS composites showed remarkable incidence of matrix attachment at fibre surface. This was associated with weak low-density binder and good fibre–matrix adhesion. As a correlation with macrostructure behaviour, those characteristics could signalise the high toughness of such composites in civil construction applications.

BSE images and EDS analyses confirmed the fibre–matrix transition zone can be improved by using production processes based on vacuum de-watering and pressure. For hydration ages ranging from approximately 60–250 days high porosity was not detected in the interfacial area and just one EDS spot indicated the presence of calcium hydroxide close to the fibres.

The partial fibre debonding and matrix cracking commonly appearing at interfacial areas should be accepted as a desirable situation for energy dissipation. Filament lumen was found free from hydration products with no evidence of fibre embrittlement under air-cure conditions at the observed ages.

Acknowledgements

Appreciation is extended to Ms. A. Pereira for her skilful assistance with sample preparation. To Mr. J.V. Ward and Mr. M. Greaves, from Ian Wark Laboratories—CSIRO, for the provision of microscopy facilities. To the Financiadora de Estudos e Projetos (Finep)—Habitare Program, the Conselho Nacional de Desenvolvimento Científico e Tecnológico (CNPq), the Coordenação de Aperfeiçoamento de Pessoal de Nível Superior (Capes, Procad) and the Fundação de Amparo a Pesquisa do Estado de São Paulo for their financial support.

References

[1] Soroushian P, Shah Z, Won J-P. Optimization of wastepaper fiber–cement composites. ACI Mater J 1995;92(1):82–92.
[2] Savastano Jr H, Warden PG, Coutts RSP. Potential of alternative fibre cements as buildings materials. Cem Concr Comp 2003;25(6):585–92.
[3] Agopyan V, John VM. Durability evaluation of vegetable fibre reinforced materials. Build Res Inform 1992;20(4):233–5.
[4] Coutts RSP. Wood fibre reinforced cement composites. In: Swamy RN, editor. Natural fibre reinforced cement and concrete. Concrete technology and design, 5. Glasgow: Blackie; 1988. p. 1–62.
[5] Savastano Jr H, Agopyan V. Transition zone studies of vegetable fibre–cement paste composites. Cem Concr Comp 1999;21(1): 49–57.
[6] Bentur A, Akers SAS. The microstructure and ageing of cellulose fibre reinforced cement composites cured in a normal environment. Int J Cem Comp Lightweight Concr 1989;11(2):99–109.
[7] Coutts RSP. Fibre–matrix interface in air-cured wood-pulp fibre–cement composites. J Mater Sci Lett 1987;6(2):140–2.
[8] Oliveira CTA, John VM, Agopyan V. Pore water composition of activated granulated blast furnace slag cements pastes. In: Proceedings 2nd International Conference on Alkaline Cements and Concretes. Kiev: Kiev State Technical University of Construction and Architecture; 1999. 9 p.
[9] Zhu WH, Tobias BC, Coutts RSP, Langfors G. Air-cured banana–fibre–reinforced cement composites. Cem Concr Comp 1994;16(1):3–8.
[10] Coutts RSP, Warden PG. Sisal pulp reinforced cement mortar. Cem Concr Comp 1992;14:7–21.
[11] Savastano Jr H, Mabe I, Devito RA. Fiber cement based composites for civil construction. In: Proceedings 2nd International Symposium on Natural Polymers and Composites—ISNaPol 98. São Carlos: Unesp/Embrapa/USP, 1998. p. 119–22.
[12] Eusebio DA, Cabangon RJ, Warden PG, Coutts RSP. The manufacture of wood fibre reinforced cement composites from Eucalyptus pellita and Acacia mangium chemithermomechanical pulp. In: Proceedings 4th Pacific Rim Bio-Based Composites Symposium. Bogor: Bogor Agricultural University; 1998. p. 428–36.
[13] Coutts RSP, Kightly P. Bonding in wood fibre–cement composites. J Mater Sci 1984;19:3355–9.
[14] Agopyan V, Savastano Jr H. Fibre–cement paste transition zone. In: Agopyan Diamond S, Savastano Jr Mindess S, Glasser FP, Roberts LW, Skalny JP, Wakeley LD, editors. Proceedings Materials Research Society Symposium on Microstructure of Cement-based Systems/Bonding and Interfaces in Cementitious Materials. MRS Symposium Proceedings, vol. 370. Pittsburgh: MRS; 1994. p. 479–86.
[15] Scrivener KL. The microstructure of concrete. In: Skalny JP, editor. Materials science of concrete I. Westerville: American Ceramic Society; 1989. p. 127–61.

[16] Kjellsen KO, Detwiler RJ, Gjorv OE. Backscattered electron image analysis of cement paste specimens: specimen preparation and analytical methods. Cem Concr Res 1991;21(2/3): 388–90.
[17] Taylor HFW. Cement chemistry. 2nd ed. London: Thomas Telford; 1997.
[18] McKenzie AW. A guide to pulp evaluation. Melbourne: CSIRO; 1994.
[19] Gram H-E. Durability of natural fibres in concrete. In: Swamy RN, editor. Natural fibre reinforced cement and concrete. Concrete technology and design, 5. Glasgow: Blackie; 1988. p. 143–72.
[20] Coutts RSP. Banana fibres as reinforcement for building products. J Mater Sci Lett 1990;9:1235–6.
[21] Savastano Jr H, Warden PG, Coutts RSP. Brazilian waste fibres as reinforcement for cement based composites. Cem Concr Comp 2000;22(5):379–84.